DNA Damage in Peripheral Blood Lymphocytes of Thyroid Cancer Patients after Radioiodine Therapy

Uta Eberlein*[1], Harry Scherthan*[2], Christina Bluemel[1], Michel Peper[2], Constantin Lapa[1], Andreas Konrad Buck[1], Matthias Port[2], Michael Lassmann[1]

[1]Department of Nuclear Medicine, University of Würzburg, Germany

[2]Bundeswehr Institute of Radiobiology affiliated to the University of Ulm,

Munich, Germany

* UE and HS equal contribution

Short title: DNA damage in Radioiodine Therapy of DTC

Corresponding author:

Michael Lassmann, PhD
Department of Nuclear Medicine
University Hospital Würzburg
Oberdürrbacher Str. 6
97080 Würzburg
Germany
Phone: +49 - 931-20135410
Email: Lassmann_m@ukw.de

Word Count: 5040

ABSTRACT

Objectives: The aim of the study was to investigate DNA double strand break (DSB) formation and its correlation to the absorbed dose to the blood in patients with surgically-treated differentiated thyroid cancer undergoing their first radioiodine therapy for remnant ablation.

Methods: 20 patients were included in this study. At least 7 peripheral blood samples were obtained before, and between 0.5h and 120h post administration of radioiodine. From the time-activity curves of the blood and the whole body, residence times for the blood self-irradiation and the irradiation from the whole body were determined. Peripheral blood lymphocytes were isolated, ethanol-fixed and subjected to immunofluorescence staining for colocalizing γ-H2AX/53BP1 DSB-marking foci. The average number of DSB foci/cell per patient sample was analyzed as a function of the absorbed dose to the blood and compared to an *in-vitro* calibration curve for ^{131}I and ^{177}Lu established previously in our institution.

Results: The average number of radiation-induced foci (RIF)/cell increased over the first 3 hours post radionuclide administration and decreased thereafter. A linear fit from 0–2 h as a function of the absorbed dose to the blood agreed with our *in-vitro* calibration curve. At later time points RIF numbers diminished, indicating successful DNA repair. Individual patient data were characterized by a linear dose-dependent increase and a biexponential response function describing a fast and a slow repair component.

Conclusions: With the experimental results and model calculations presented in this work, a dose-response relationship is demonstrated and an analytical function describing the time course of the *in-vivo* damage response after internal irradiation of patients with ^{131}I is established.

Key words: γ-H2AX, 53BP1, biological dosimetry, radioiodine therapy, DTC, absorbed dose to blood, DSB focus assay, DNA damage, ^{131}I, differentiated thyroid cancer

INTRODUCTION

Following total thyroidectomy for differentiated thyroid cancer (DTC), patients generally receive one or more treatments with high activities of [131]I. The purpose of the initial radioiodine therapy after surgery is to ablate remnant thyroid tissue and to effectively treat any iodine-avid metastases *(1,2)*. As patients with DTC generally do not undergo chemotherapy or other radiotherapy prior to radioiodine therapy, this patient group is ideally suited for the investigation of the DNA damage in blood lymphocytes after protracted, nearly homogeneous whole-body irradiation. In this setting, all organs, including the blood, are irradiated by β-particles emitted from circulating ^{131}I and from penetrating γ-radiation originating from activity dispersed throughout the body. The absorbed dose and dose rate to the blood is assessed by defining the time–activity curves in the blood and the whole body, integrating the corresponding time-activity curves and calculating the absorbed dose according to European Association of Nuclear Medicine (EANM) standard operating procedure (SOP) for DTC *(3)*.

Ionizing radiation (IR) does not only destroy the malignant iodine avid cells, it can also damage healthy tissues and cells. Among the elicited damage, DNA double-strand breaks (DSBs) are the most crucial lesions for the healthy tissue because their repair is difficult and faulty DNA repair leads to mutations, chromosomal aberrations or cell death.

In general, DSBs evoke a DNA damage response during which the DSB signal is amplified and several repair routes are induced that involve proteins that can serve as biomarkers*(4)*.

The formation of a DSB in nuclear chromatin results in the rapid phosphorylation of the histone H2 variant H2AX, then called γ-H2AX *(5–7)*. Furthermore, DSBs also recruit the damage sensor protein 53BP1 to the chromatin around DSBs *(8–12)*, which leads to 53BP1 and γ-H2AX co-localization in the chromatin surrounding a DSB *(8,10,13–15)*. By immunofluorescence (IF) staining with γ-H2AX and 53BP1 antibodies those biomarkers can be addressed as microscopically visible fluorescent foci *(14–16)*. With progression of DSB repair, γ-H2AX and 53BP1 foci disappear *(17)*.

At present, there are only two studies that quantified radiation-induced DNA damage foci formation after therapy of differentiated thyroid cancer (DTC) with the isotope ^{131}I, either using radiation-induced co-localizing γ-H2AX and 53BP1 foci *(18)* or γ-H2AX foci alone*(19)*. More

recent studies addressed γ-H2AX foci formation after ^{177}Lu therapy of neuroendocrine tumors *(16,20)*. In these studies the authors observed elevated levels of radiation-induced DNA damage foci after treatment, but a clear dose-response relationship could only be established in one study *(16)*.

The aims of the present study were therefore, a) to compare the *in-vivo* dose response in the first hours after therapy to an *in-vitro* calibration curve established recently in our laboratory *(15)*, and b) to describe the temporal and dose-dependent behavior of the radiation-induced foci (RIF) in radiation treatment-naïve patients after their first radioiodine therapy (RIT) with [131]I.

MATERIALS AND METHODS

Research Design and Subjects

Patients referred to our center for initial treatment with radioiodine after surgery for differentiated papillary or follicular thyroid carcinoma were included in this study. Before treatment, each patient received 3-8MBq of ^{131}I for thyroid bed tracer uptake measurement to screen for thyroid remnants large enough to require re-operation. Patients with a 24h iodine uptake of more than 5% in the thyroid bed were excluded from the study. Higher uptake in the thyroid bed would affect the dosimetry calculations. No patient had a history of leukemia or lymphoma, radio- or chemotherapy; none underwent an X-ray examination or, other than the remnant tracer uptake measurement, scintigraphy within ≤3 months before radioiodine therapy. The research plan was presented to the ethics committee of the Medical Faculty of the University of Würzburg (Az: 112/11). The ethics committee approved the study by stating that there were no objections to the conduct of the study. Prior to the study, all patients gave their written informed consent. For treatment, the patients were hospitalized for at least 48 hours, normally up to 3-4 days.

Blood sampling and activity determination of blood samples

Blood samples were drawn in all patients prior to administration and nominal at 0.5h, 1h, 2h, 3h, 4h, 24h, 48h and up to 168h after administration using Li-Heparin blood collecting tubes (S-Monovette, Sarstedt, Germany). For an exact quantification of the blood activity concentration, an aliquot of 0.1mL of each heparinized blood sample was measured in a well counter (Canberra, Germany) or in a high-purity germanium detector (Canberra, Germany). The counting efficiencies of both detectors were determined by repeated measurements of a NIST-traceable standard. The measured values were decay-corrected to the time of blood drawing. The statistical error of the activity determination was less than 1% for the blood samples taken at the first day. The statistical error increased for later time points, but was always less than 5%.

Blood sample preparation for the DNA damage focus assay

The separation and fixation of the white blood cells and the counting of the identified DSB foci followed the protocol described in detail in Eberlein et al. *(16)* and the DSB foci staining was performed according to Lassmann et al. *(18)* and Lamkowski et al. *(14)*. Briefly, white blood cells were obtained by density centrifugation (CPT Vacutainer tube, BD, Germany) and fixed in ice-cold 70% Ethanol. Samples were kept at -20°C until immunostaining for γ-H2AX and 53BP1 using primary antibodies against γ-H2AX (Millipore) and 53BP1 (Acris Antibodies) that were detected with secondary goat anti-mouse Alexa-488 and donkey anti-rabbit Cy3-labeled antibodies (both Dianova), respectively. The number of DSB repair protein foci was analysed by an experienced investigator (HS) in lymphocyte nuclei (n=100 peripheral blood lymphocytes/sample) by manual focus counting using a red/green double band pass filter (AHF) and 63x lens of a Zeiss Axioimager 2i fluorescence microscope equipped with the ISIS fluorescence imaging system (MetaSystems).

Counting the blood sample before therapy gave us the baseline, background foci rate. This rate was subtracted from the DNA foci count rates obtained after irradiation, which resulted in the average number of RIF per cell.

Measurement of the whole-body retention

Whole body activity retention was determined in all patients by external dose rate measurements according to the methodology described by the EANM SOP for patients with DTC

(3). Dose-rate measurements were performed by use of a ceiling-mounted shielded survey meter (automess GmbH, Germany) at a fixed distance of 2.5m above the patients' beds. The first patient measurement was carried out immediately after administration (approximately 15 minutes after ^{131}I application) and at least two times per day thereafter. Data were normalized to the first measurement.

Calculation of the time-integrated activity coefficients and the absorbed doses

The calculation of the time-dependent time-integrated activity coefficients for the total body (tb) (τ_{tb} (t)) and the blood (bl) ($\tau_{ml\ of\ bl}$ (t)) and the absorbed doses ($\overline{D}_{bld}(t)$) after administration of ^{131}I were performed according to the EANM SOP *(3)* and as described previously *(16)*. These coefficients are obtained by integrating the respective time-activity curve from 0 to the time point t (instead of infinity). Since we took multiple blood samples and measured the retention of the whole-body up to 168h after therapy, the corresponding time-activity curves for ^{131}I were fitted by bi- or tri-exponential functions.

As the activity was administered orally, the iodine washout from the stomach to the blood circulation needs to be taken into account. According to Leggett *(21)* the iodine uptake is 5% per minute. Therefore, we assumed a linear iodine uptake within the first 20 minutes for the time activity curve of the blood and the bi- or tri-exponential fits were performed from t=20 min. The absorbed dose $\overline{D}_{bl}$ (t) after 20 minutes was calculated as follows:

$$\overline{D}_{bl}\ (t) = A_0 \cdot \left(108\ \frac{\text{Gy} \cdot \text{ml}}{\text{GBq} \cdot \text{h}} \cdot \tau_{ml\ of\ bl}\ (t) + \frac{0.0188}{wt^{\frac{2}{3}}}\frac{\text{Gy} \cdot \text{kg}^{\frac{2}{3}}}{\text{GBq} \cdot \text{h}} \cdot \tau_{tb}(t) \right) \tag{1}$$

A_0 denotes the administered activity and *wt* represents the patient's weight in kg.

Modelling the time-dependency of the focus induction and disappearance

The modelling of the time-dependency of the DSB focus induction and disappearance followed the method described previously *(16)*. The number of RIF/cell as a function of the time-dependent absorbed dose and the disappearance of the foci are described in the early hours of treatment by a linear dose-dependent increase, with the parameters taken from our *in-vitro* calibration curve *(15)* and a bi-exponential decay representing DNA repair:

$$N(t) = \left(a + m \cdot b \cdot \overline{D}_{bl}(t)\right) \cdot \left(k \cdot e^{-\lambda \cdot t} + (1-k) \cdot e^{-\upsilon \cdot t}\right) \qquad (2)$$

N(t): number of RIF/cell at time *t*

a,b: Constants taken from the in-vitro calibration curve *(15)*; they describe the number of RIF/cell as a linear function of the time-dependent mean absorbed dose $\overline{D}_{bl}(t)$ (a=0.0363 RIF/cell; b=0.00147 RIF/cell·mGy^{-1}). The in-vitro calibration curve was generated with blood samples of volunteers that were irradiated internally with ^{131}I and ^{177}Lu with absorbed doses up to 100 mGy. The number of RIF/cell increased linearly with the absorbed dose to the blood.

m: Adjustable parameter to account for the variability in the patient dosimetry with respect to the linear *in-vitro* calibration function *(15)*.

k: Adjustable parameter describing the fraction of damage assigned to different repair rates.

λ, υ: Patient-specific adjustable parameter describing the decay rate of foci.

Statistics

Origin (Version 9.1G+2015G, Origin Lab Corporation) was used for data analysis and statistical evaluation. Normal distribution of the data sets was tested using the Shapiro-Wilk test. Changes in RIF/cell values sets at different time points were compared by the paired Wilcoxon signed-rank test. Differences are considered to be significant if $p<0.05$.

RESULTS

Patients

Twenty patients (8 male / 12 female) with a mean age of 55.1±17.1 years were recruited and included in this study. More details on the patients' demographics are given in supplemental Table S1. Most of the patients (n=16) presented with papillary thyroid cancer. The patients received a mean of 3.5±0.3GBq ^{131}I-iodide for their first therapy. All patients except one (P35) were treated while being hypothyroid.

Thereafter, patients were admitted to our ward and hospitalized for at least three days (15 patients) or even more until the external dose rate dropped below 3.5µSv/h at a distance of

2.5m during their hospital stay. The majority of the blood samples and measurements were taken during this time period. For some patients, final blood withdrawal and dose rate measurements were performed when they were scheduled for their final post-therapeutic gamma camera imaging. All patients responded well to the treatment or showed disease stabilization at follow-up. No therapy or study-related adverse events were observed.

DNA Damage Foci

Peripheral blood lymphocytes were stained immunofluorescently for γ-H2AX and 53BP1 *(14,18)*. DNA damage foci were manually enumerated for co-localizing γ-H2AX/53BP1 DSB-marking foci. Average numbers of RIF per cell were calculated for each patient sample (figure 1) as a function of time after administration of the radiopharmaceutical. The average number of RIF/cell increased in the first hours after therapy, declining at later time points (figure 1, Table 1). The actual time points differed slightly because of variations in the individual patient management. The mean number of foci varied between 0.50±0.14RIF/cell at t=4h, 0.31±0.10RIF/cell at t= 24h, and 0.18±0.09RIF/cell at t=48h after administration of [131]I.

Only datasets of 4h and 48h were distributed according to a Gaussian distribution (Shapiro Wilk test). Therefore, we chose a non-parametric test (Wilcoxon signed-rank test) to compare the datasets at 4h, 24h and 48h. Applying the Wilcoxon signed-rank test to those time points revealed that there was a statistically significant decrease between the number of RIF/cell at these time points ($p < 0.05$) confirming the observation that the number of RIF/cell declined 5 h after administration of the radiopharmaceutical (see figure 1).

Dosimetry

The absorbed doses to the blood for the individual patients were calculated according to the EANM SOP(3). The mean absorbed dose was 66±17mGy at t=4h, 205±49mGy after 24h, 263±63mGy after 48h, and the total absorbed dose after administration was 367±105mGy (Table 1). The specific total absorbed dose to the blood in all hypothyroid patients was 100±22mGy/GBq. This value is in good agreement with the value of 93± 35mGy/GBq found in our previous study (18), further confirming the validity of the method.

The absorbed dose to the blood increased steeply in the first few hours after therapy (figure 2A). In most patients, 50% of the total absorbed dose to the blood was reached within the first 24 hours (figure 2B). In accordance with this observation, the dose-rate declined until it was ≤0.5mGy/h after 80h. For overview, figure 3 shows the average RIF/cell values of an exemplary patient (P45) as a function of the absorbed dose to the blood.

In-vivo calibration of the DNA damage focus assay

A fit within the first 4-5 hours as performed in the publication with ^{177}Lu patients *(16)* after administration of the radioactivity could not be performed. The reason was the observation of a slower increase of the number of RIF/cell after 2 h. For the in-vivo calibration, therefore, only the first 2 hours after administration of the radioactivity or the first two data points were considered. Those datasets were pooled and the average number of RIF/cell as a function of the absorbed dose were fitted linearly:

$$y = 0.0064 \cdot \text{RIF/cell} + 0.0117 \cdot \text{RIF/cell} \cdot \text{mGy}^{-1} \cdot x \qquad (3)$$

y denotes the number of RIF/cell and x the absorbed dose to the blood in mGy ($R^2 = 0.86$). The standard error of the y-axis intercept is ±0.0089 RIF/cell and the standard error of the slope is ±0.0006 RIF/cell mGy^{-1}. The resulting *in-vivo* calibration curve for our experiments including a 95% confidence interval is shown in figure 4 in black.

In a previous study we obtained an *in-vitro* calibration in blood samples of volunteers for ^{131}I and [177]Lu *(15)*. For comparison, this *in-vitro* calibration curve is shown in red in figure 4. The slope for the patient data is smaller with a relative deviation of the slopes of 20% between the *in-vitro* calibration and the *in-vivo* data.

Compared to the fit of the ^{177}Lu patients *(16)*, the [131]I *in-vivo* fit has a slope which is 7.9% lower. This is most likely caused by the early onset of a fast DNA damage repair component in the ^{131}I patients.

Modeling

Individual fits of the patient foci data after the first RIT were performed according to eq. 2 using the datasets for the biokinetics of blood and whole-body. Variable parameters to be fitted were m, λ, k and v (Table 2). The bi-exponential fit converged for 12 patients. Three patients

showed a very fast decay of the number of RIF/cell (P40, P42, P44). For these patients the fit did not converge. Three patients (P30, P33, P39) were released from the ward 48h after administration, therefore, blood samples could not be taken at later time points, and, consequently, a bi-exponential fit was impossible. For patients P37 and P47 a mono-exponential decay represented the RIF/cell data better although their blood samples were taken at time-points ≥48h; the mean values including their standard deviations were taken from the 12 patients for whom the fit converged and had three or more data points ≥24h (Table 2).

In general, the data followed a straight line for the first 1-2 hours after ^{131}I administration. The mean value of the fit parameter m, which accounts for the variability in the patient dosimetry with respect to the *in-vitro* calibration, was 1.10±0.53 (minimum 0.56, maximum: 2.50). The mean (fast) decay rate (λ) for all 12 patients was $0.325±0.128h^{-1}$ (minimum: $0.15h^{-1}$, maximum: $0.66h^{-1}$). The (slow) decay rate v ranged from $0.01h^{-1}$ to $0.08h^{-1}$ (mean: $0.040±0.020h^{-1}$). The mean value for k was 0.758±0.129 indicating that about 76% of the DNA damage is repaired with a high decay rate. Expressed as half-lives the mean values of the fast decay is $T_{fast}=2.1h$ and $T_{slow}=17.3h$.

The time-dependent response function (equation 2) shown in figure 5 (green curve) is based on the mean parameters provided in table 2. According to this function the highest number of RIF/cell can be expected 3.2 hours after administration of [131]I. After 148h the mean DSB foci values drop below the maximum standard deviation of the background RIF/cell value of 0±0.04 RIF/cell. The standard deviation of the background foci includes the counting error, therefore each data point is considered with appropriate error propagation, even the baseline value of the RIF/cell at 0mGy. This means that some patients still have slightly elevated numbers of RIF, even up to 4 days after treatment started.

DISCUSSION

There is a limited number of publications investigating the effect of DSB induction after radionuclide therapy or diagnostics *(16,18–20,22)*. However, nuclear medicine treatments involve systemic internal irradiation as compared to external irradiation (e.g., in radiotherapy). After nuclide incorporation the cells are irradiated by internalized and extracellular ^{131}I not only

for seconds or minutes but are continuously irradiated over a longer period with permanently changing dose rate. This could alter the effect of radiation damage compared to a fractionated high dose rate partial body irradiation in radiotherapy. In a previous peptide receptor radionuclide therapy (PRRT) study with ^{177}Lu we reported a first linear relationship between the number of RIF/cell and the absorbed dose to the blood only over the first 4 to 5 hours after therapy start (16). After this period, the disappearance of the DSB foci was reflected by the decay of the RIF/cell numbers.

This study with ^{131}I showed a similar relationship; however, the time period of the linear dependence was reduced to 2 hours after administration of the β-emitter ^{131}I (see figure 1B) indicating a faster decay of the RIF/Cell number. The time points after 2h were characterized by a diminishing number of radiation-induced foci in accordance with the progression of DNA repair and the declining dose rates. This finding agrees well with our previous studies that showed the highest value of RIF/cell at early time-points with subsequent, statistically significant reduction of the of RIF/cell numbers at later time-points (16,18).

Analysis of γ-H2AX/53BP1 foci kinetics in peripheral blood lymphocytes of 16 patients undergoing PRRT (16) revealed, however, likely due to the short time period of measurement after therapy (< 48h), only a mono-exponential decay curve (16). Compared to our previous study in patients after PRRT there is a deviation from a straight line in this study at time points ≥2h after ^{131}I administration. This might be caused by the higher mean absorbed dose imparted to the blood in the first hour after treatment (14±5 mGy for ^{177}Lu PRRT*, 23±8 mGy for ^{131}I RIT). This effect mirrors the one for the differential foci response of human fibroblasts after irradiation with X-rays for absorbed doses >10mGy (23).

The disappearance of RIF/cell as a function of time has been quantitatively described by Horn et al. (24), Mariotti et al. (25) and Eberlein et al. (16). The values reported in this study for the slow and fast component of decay were in good agreement with the findings of Horn et al. (24), characterizing the disappearance of RIF/cell by a bi-exponential response function with a short decay rate of 0.35h^{-1} (77%) and a longer-lived component of 0.018h^{-1} (23%). The range of our RIF/cell decay rate for the fast component is within the value ranges of Horn et al. (24) and Mariotti (25) (0.23h^{-1}). The slow decay component by Mariotti et al. does not contribute greatly

---

* Unpublished data taken from our PRRT study

to the decay of RIF/cell (probability: 9%) and is $<10^{-11}h^{-1}$. Most likely, their way of irradiating the cells does not compare to our case of continuous internal irradiation with decreasing dose rate.

Several RIT patients showed a fast mono-exponential decay rate, pointing at the fact that their DSB repair could have been more effective as compared to the other patients. However, for these patients no obvious link between this finding and the pre-treatment or stage of the disease could be found.

Further studies with more patients, other isotopes and/or radiopharmaceuticals showing different kinetics of the tracer in the blood are needed to better identify repair kinetics and patients with different repair rates.

CONCLUSIONS

This study describes the kinetics of ^{131}I incorporation-induced DSBs in blood lymphocytes during radioiodine therapy as a function of the absorbed dose to the blood. In the first hours after therapy the number radiation-induced DSBs per cell increased linearly with the absorbed dose and mirrored our recently established in-vitro calibration curve. At more advanced time-points after administration of the radiopharmaceutical, the induction of a fast and a slow repair component of the double-stranded DNA damage was seen. In this study, we found a dose-dependent analytical function describing the internal ^{131}I irradiation-induced time course of induction and decay of DSB foci in RIT patients.

REFERENCES

1. Luster M, Clarke SE, Dietlein M et al. Guidelines for radioiodine therapy of differentiated thyroid cancer. *Eur J Nucl Med Mol Imaging*. 2008;35:1941–1959.
2. American Thyroid Association (ATA) Guidelines Taskforce on Thyroid Nodules and Differentiated Thyroid Cancer, Cooper DS, Doherty GM et al. Revised American Thyroid Association management guidelines for patients with thyroid nodules and differentiated thyroid cancer. *Thyroid*. 2009;19:1167–1214.
3. Lassmann M, Hänscheid H, Chiesa C, Hindorf C, Flux G, Luster M. EANM Dosimetry Committee series on standard operational procedures for pre-therapeutic dosimetry I: blood and bone marrow dosimetry in differentiated thyroid cancer therapy. *Eur J Nucl Med Mol Imaging*. 2008;35:1405–1412.
4. Manning G, Rothkamm K. Deoxyribonucleic acid damage-associated biomarkers of ionising radiation: current status and future relevance for radiology and radiotherapy. *Br J Radiol*. 2013;86:20130173.
5. Rogakou EP, Pilch DR, Orr AH, Ivanova VS, Bonner WM. DNA double-stranded breaks induce histone H2AX phosphorylation on serine 139. *J Biol Chem*. 1998;273:5858–5868.
6. Rothkamm K, Löbrich M. Evidence for a lack of DNA double-strand break repair in human cells exposed to very low x-ray doses. *Proc Natl Acad Sci U S A*. 2003;100:5057–5062.
7. Ivashkevich A, Redon CE, Nakamura AJ, Martin RF, Martin OA. Use of the γ-H2AX assay to monitor DNA damage and repair in translational cancer research. *Cancer Lett*. 2012;327:123–133.
8. Schultz LB, Chehab NH, Malikzay A, Halazonetis TD. p53 binding protein 1 (53BP1) is an early participant in the cellular response to DNA double-strand breaks. *J Cell Biol*. 2000;151:1381–1390.
9. Anderson L, Henderson C, Adachi Y. Phosphorylation and rapid relocalization of 53BP1 to nuclear foci upon DNA damage. *Mol Cell Biol*. 2001;21:1719–1729.
10. Rappold I, Iwabuchi K, Date T, Chen J. Tumor suppressor p53 binding protein 1 (53BP1) is involved in DNA damage-signaling pathways. *J Cell Biol*. 2001;153:613–620.
11. Huyen Y, Zgheib O, DiTullio Jr RA et al. Methylated lysine 79 of histone H3 targets 53BP1 to DNA double-strand breaks. *Nature*. 2004;432:406–411.
12. Panier S, Boulton SJ. Double-strand break repair: 53BP1 comes into focus. *Nat Rev Mol Cell Biol*. 2014;15:7–18.
13. Ward IM, Minn K, Jorda KG, Chen J. Accumulation of Checkpoint Protein 53BP1 at DNA Breaks Involves Its Binding to Phosphorylated Histone H2AX. *J Biol Chem*. 2003;278:19579–19582.
14. Lamkowski A, Forcheron F, Agay D et al. DNA Damage Focus Analysis in Blood Samples of Minipigs Reveals Acute Partial Body Irradiation. *PLoS ONE*. 2014;9:e87458.
15. Eberlein U, Peper M, Fernández M, Lassmann M, Scherthan H. Calibration of the γ-H2AX DNA Double Strand Break Focus Assay for Internal Radiation Exposure of Blood Lymphocytes. *PLoS ONE*. 2015;10:e0123174.
16. Eberlein U, Nowak C, Bluemel C et al. DNA Damage in Blood Lymphocytes in Patients after Lu-177 Peptide Receptor Radionuclide Therapy. *Eur J Nucl Med Mol Imaging*. 2015;42:1739–1749.

17. Chowdhury D, Keogh M-C, Ishii H, Peterson CL, Buratowski S, Lieberman J. γ-H2AX Dephosphorylation by Protein Phosphatase 2A Facilitates DNA Double-Strand Break Repair. *Mol Cell*. 2005;20:801–809.

18. Lassmann M, Hänscheid H, Gassen D et al. In vivo formation of gamma-H2AX and 53BP1 DNA repair foci in blood cells after radioiodine therapy of differentiated thyroid cancer. *J Nucl Med*. 2010;51:1318–1325.

19. Doai M, Watanabe N, Takahashi T et al. Sensitive immunodetection of radiotoxicity after iodine-131 therapy for thyroid cancer using γ-H2AX foci of DNA damage in lymphocytes. *Ann Nucl Med*. 2013;27:233–238.

20. Denoyer D, Lobachevsky P, Jackson P, Thompson M, Martin OA, Hicks RJ. Analysis of ^{177}Lu-Octreotate Therapy–Induced DNA Damage in Peripheral Blood Lymphocytes of Patients with Neuroendocrine Tumors. *J Nucl Med*. 2015;56:505–511.

21. Leggett RW. A physiological systems model for iodine for use in radiation protection. *Radiat Res*. 2010;174:496–516.

22. May M, Brand M, Wuest W et al. Induction and repair of DNA double-strand breaks in blood lymphocytes of patients undergoing ^{18}F-FDG PET/CT examinations. *Eur J Nucl Med Mol Imaging*. 2012;39:1712–1719.

23. Grudzenski S, Raths A, Conrad S, Rübe CE, Löbrich M. Inducible response required for repair of low-dose radiation damage in human fibroblasts. *Proc Natl Acad Sci U S A*. 2010;107:14205–14210.

24. Horn S, Barnard S, Rothkamm K. Gamma-H2AX-based dose estimation for whole and partial body radiation exposure. *PloS One*. 2011;6:e25113.

25. Mariotti LG, Pirovano G, Savage KI et al. Use of the γ-H2AX Assay to Investigate DNA Repair Dynamics Following Multiple Radiation Exposures. *PLoS ONE*. 2013;8:e79541.

Table 1: Number of RIF/cell and absorbed doses to the blood at different time points

Patient ID	Background foci values	Absorbed Dose (mGy) t=4h§	# of RIF/cell t=4h§	Absorbed Dose (mGy) t=24h§	# of RIF/cell t=24h§	Absorbed Dose (mGy) t=48h§	# of RIF/cell t=48h§	Total Absorbed Dose (mGy)
P27	0.024	98	0.650	284	0.310	344	0.240	366
P29	0.020	52	0.460	139	0.310	169	0.110	299
P30	0.045	53	0.240	208	0.400	331	0.260	594
P31	0.024	51	0.390	163	0.410	203	0.170	370
P32	0.028	72	0.510	252	0.360	340	-	429
P33	0.047	98	0.560	270	0.370	328	0.210	350
P34	0.042	61	0.370	199	0.280	262	0.120	301
P35	0.040	59	0.340	149	0.390	203	0.300	665
P36	0.020	69	0.730	225	0.380	272	0.260	315
P37	0.020	55	0.410	186	0.290	231	0.070	340
P38	0.032	56	0.350	195	0.300	269	0.230	322
P39	0.024	60	0.360	156	0.140	207	0.050	256
P40	0.063	69	0.700	208	0.120	254	0.130	420
P41	0.037	86	0.540	265	0.280	347	0.220	401
P42	0.014	79	0.670	214	-	263	0.240	285
P43	0.035	92	0.630	286	0.370	363	0.210	418
P44	0.071	57	0.380	192	0.050	230	0.000	269
P45	0.035	63	0.640	205	0.390	264	0.170	380
P46	0.042	37	0.500	112	0.300	138	0.320	275
P47	0.079	56	0.520	183	0.390	247	0.100	286
MEAN	0.037	66	0.498**	205	0.307**	263	0.179**	367
SD	0.004	17	0.137	49	0.099	63	0.085	105

**Statistically significant differences (p< 0.008), §Nominal time points, SD: standard deviation

Table 2: Individual fit parameters for equation 2

Patient ID	m	λ	k	v
		h^{-1}		h^{-1}
P27	1.010	0.284	0.883	0.034
P29	1.868	0.659	0.723	0.080
P30*	0.338	0.058	1	-
P31	1.050	0.414	0.520	0.058
P32	0.750	0.207	0.782	0.035
P33*	0.524	0.072	1	-
P34	0.657	0.215	0.542	0.051
P35	0.949	0.365	0.825	0.010
P36	1.027	0.281	0.945	0.015
P37**	0.639	0.083	1	-
P38	0.728	0.260	0.673	0.036
P39*	0.461	0.098	1	-
P40	fit did not converge			
P41	1.254	0.428	0.837	0.056
P42	fit did not converge			
P43	0.566	0.153	0.790	0.026
P44	fit did not converge			
P45	1.335	0.301	0.683	0.056
P46	2.504	0.336	0.896	0.020
P47**	0.875	0.076	1	-
Mean	1.101	0.325	0.758	0.040
SD	0.532	0.128	0.129	0.020
Median	1.019	0.293	0.786	0.036

* Latest time point: 48h

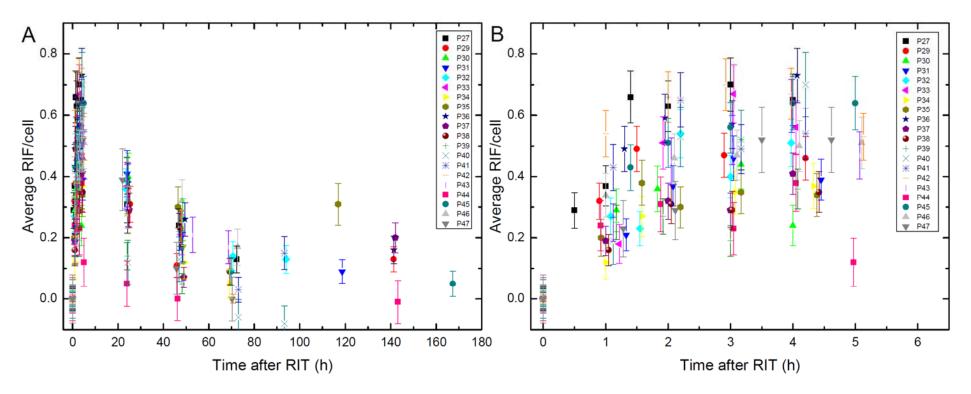** For these patients a mono-exponential function described the RIF/cell data best

Figure 1: Average RIF/cell as a function of time after administration of ^{131}I for time points 0h-168h (A) and a detailed view of time points 0h-5h (B).
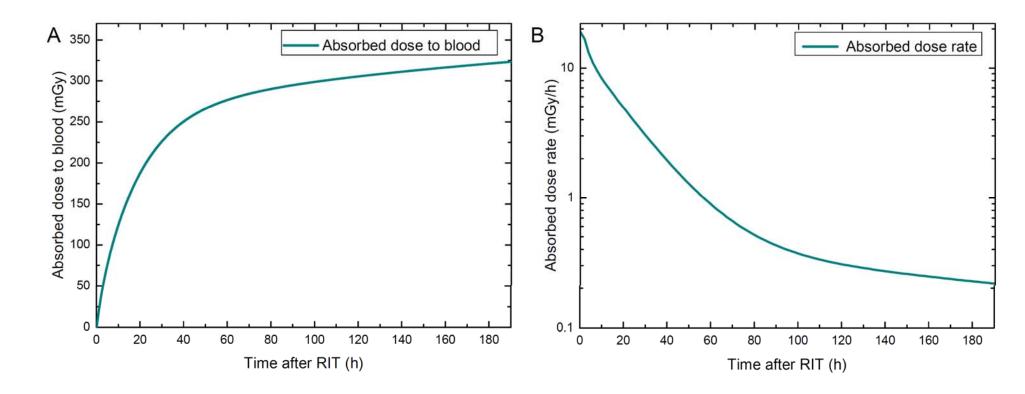
Figure 2: Absorbed dose (A) and dose rate (B) to the blood for patient P45 as a function of time
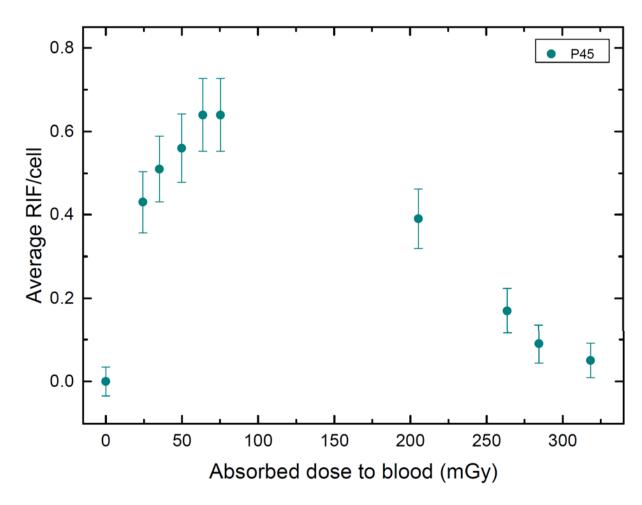
Figure 3: Average RIF/cell as a function of the absorbed dose to the blood for patient P45. The time points of the blood withdrawals were: 0h, 1.4h, 2.0h, 3.0h, 4.0h, 5.0h, 24.0h, 48.2h, 69.8h, and 167.3h.
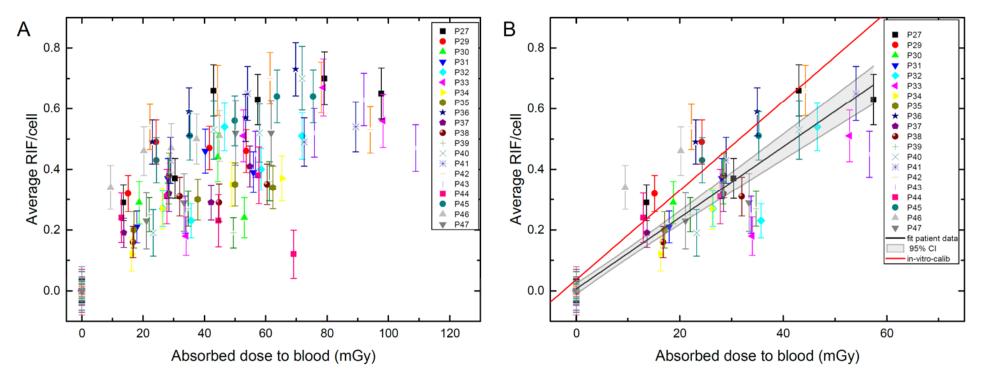
Figure 4: Average number of RIF/cell as a function of the absorbed dose to the blood (A) for the first 5 hours after ^{131}I administration and (B) for the first 2 h after administration. Black line: linear fit to our ^{131}I patient data including the 95% confidence interval (CI), Red line: in-vitro calibration. Curve taken from Eberlein et al. *(15)*
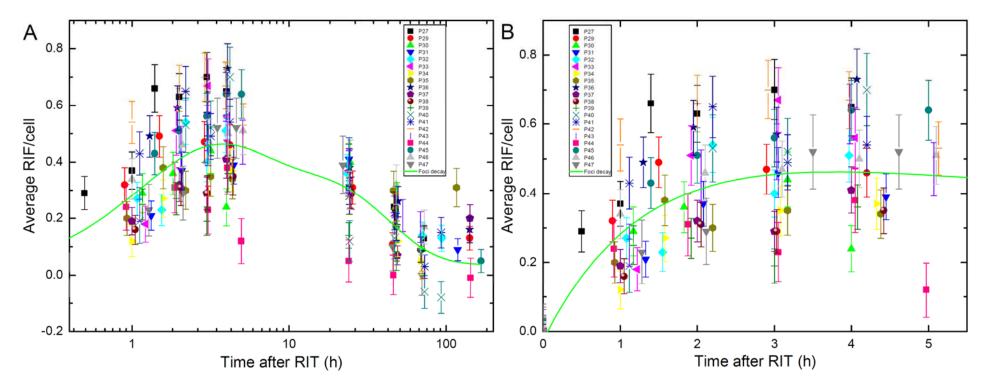
Figure 5: Average number of RIF/cell as a function of time after ^{131}I administration (A). The green curve represents the response function according to equation 2 using mean values for all parameters. The right panel (B) shows a more detailed view of the response function for the first 5 hours after ^{131}I administration.